Received 28 July 1967 13.2, 13.3

Ray Theory Applied to a Wide Class of Velocity Functions*

MELVIN A. PEDERSEN

Naval Undersea Warfare Center, San Diego, California 92152

Ray-theory expressions for the range, travel time, and intensity are developed for a newly formulated sound-velocity profile model in which the velocity is expressed as a series in integral and half-integral powers of ocean depth. By the process of series inversion, any analytic function for which the first and second depth derivatives do not vanish simultaneously can be cast into this model. The series inversion process is applied to several elementary velocity functions, demonstrating that the general function solutions reduce to ray theory solutions obtainable by direct methods. Procedures and numerical examples for fitting experimental underwater-sound-velocity data to the model are presented. Acoustic artifacts, such as artificial layering effects, can be minimized because each layer may contain an arbitrary number of parameters and because the velocity and an arbitrary number of derivatives may be matched at layer interfaces.

INTRODUCTION

THE purpose of this paper is to present the expressions necessary for the calculation of ray intensities in underwater acoustics for a very general class of mathematical function useful in the approximation of the velocity–depth profile. The only restriction on this function is that C be an analytic function of Z and that there be no point for which both the first and second depth derivatives of the velocity vanish simultaneously.

In the initial study,[1] leading to the present approach, the anomalies introduced by slope discontinuities at layer interfaces were presented. The anomalies included the generation of regions of unrealistically low intensity, the introduction of false caustics, and the omission of real caustics.

In a second study,[2] a profile approximation that preserved continuity of slope at layer interfaces was presented. Although this second approach eliminated the anomalies just discussed, artificialities introduced by layering were still present in the form of infinite rates of change in intensity. This artificiality was demonstrated to result from discontinuities in the second derivative at layer interfaces. A new profile model—the subject of the present study—was suggested as a method of eliminating all artificialities introduced by layering.

In this new model, each layer may contain an arbitrary number of parameters. Realistic profile approximations are possible using a minimal number of layers. The number of layers necessary is the number of points for which the first depth derivative of the velocity is zero. An arbitrary number of derivatives may be matched at each layer interface, and the matching of at least two is recommended.

Section I of this paper discusses the profile model and develops expressions for range, range derivatives, and travel time. Section II presents examples of how the general theory may be applied to mathematical profiles by the use of series inversion. Section III presents techniques and examples for fitting the profile model to experimental velocity data points. Section IV outlines present investigation.

I. THEORY

This section presents the profile model and develops all the expressions necessary for the computations of intensity and travel time by ray theory.

The basic nomenclature follows that of a previous paper.[1] The medium is divided into horizontal layers in which the velocity (C) is assumed to be a function of depth (Z) alone. The rays are designated by C_m, the velocity at which the ray becomes horizontal. In this method, Snell's law becomes

$$\cos\theta = C/C_m, \tag{1}$$

where θ is the angle formed by the ray with the horizontal.

* Portions of this paper were presented at the seminar on sound-ray tracing and isointensity contours in the ocean held at Pennsylvania State University on 11–14 July 1965.

[1] M. A. Pedersen, J. Acoust. Soc. Am. **33**, 465–474 (1961).

[2] M. A. Pedersen and D. F. Gordon, J. Acoust. Soc. Am. **41**, 419–438 (1967).

The horizontal range increment in Layer i is designated by R_i, associated derivatives by dR_i/dC_m and d^2R_i/dC_m^2, and corresponding travel time by T_i. The complete horizontal range R is given by $\sum R_i$, where the summation extends over all layers as traversed along the ray path from source to receiver. Corresponding values for derivatives and travel time are $dR/dC_m = \sum dR_i/dC_m$, $d^2R/dC_m^2 = \sum d^2R_i/dC_m^2$, and $T = \sum T_i$.

The desired source or receiver depths must be located at interfaces. These may be either the natural boundaries between distinct layers or additional interfaces introduced within a natural layer at the desired source and receiver depths.

The ray intensity for a unit source may be written as

$$\frac{I}{F} = \frac{C_s |\cot\theta_s| |\cot\theta_h|}{C_h C_m R |dR/dC_m|},$$

where the subscripts s and h refer to the source and receiver, respectively. F is a measure of the source strength. In the computations, it is convenient to express all velocities in yd/sec and other profile parameters in depth units of yards, for then the intensities are measured relative to 1 yd.

The remainder of this Section discusses the nature of the profile model and develops expressions for the ray theory quantities associated with Layer i.

A. Model of the Velocity–Depth Profile

The profile model treated in this paper consists of a number of layers in which the velocity and depths are related by

$$(Z - Z_0) = \sum b_n |C - C_0|^{n/p}, \tag{2}$$

where $p = 1$ or 2. This limitation in p is imposed by the fact that these are the values for which the ray theory integrals are tractable in terms of known mathematical functions. In order to treat both cases of p simultaneously, it is necessary to employ certain notation conventions. For example, in Eq. 2, and in all expressions to follow, the absolute-value symbols apply only when $p = 2$. When $p = 1$, any absolute-value symbols should be treated as if they were parentheses.

The parameters that define the profile in Layer i are Z_{0i}, C_{0i}, p_i, and the b_{ni}'s. Generally, there is a different set of parameters for each layer, the exception being the introduction of source and receiver depths within a natural layer. In order to simplify the notation, we drop the i subscripts on the profile parameters, as was done in Eq. 2. When discussing Layer i, it is understood that the parameters associated with the profile are the set for Layer i.

There are two distinct approaches to the determination of the parameters in Eq. 2. In the first approach, discussed in detail in Part III, the parameters are determined from experimental data by least-squares fits. In this case, the number of terms in Eq. 2 is a finite number, N. In the second approach, a wide class of mathematical functions may be cast into the form of Eq. 2.

Section II demonstrates that any function, C, which is analytic at Z_0, can be converted into Eq. 2, where p is the order of the first nonvanishing derivative of C with respect to Z evaluated at Z_0. Section II also presents methods by which b_n may be evaluated in terms of the derivatives of C with respect to Z evaluated at Z_0.

When $p = 1$, i.e., $(dC/dZ)_{Z_0} \neq 0$, Eq. 2 is an expansion in integral powers of $C - C_0$. When $p = 2$, the point (Z_0, C_0) is a branch point and Eq. 2 represents an expansion about a relative minimum or relative maximum in the velocity profile depending, respectively, on whether $(d^2C/dZ^2)_{Z_0}$ is positive or negative.

In developing the ray theory, expressions for the first three derivatives of Eq. 2 are necessary. Successive differentiation leads to

$$dZ/dC = \sum B_n |C - C_0|^{n/p - 1}, \tag{3}$$

$$d^2Z/dC^2 = \sum \pm B_n (n - p) p^{-1} |C - C_0|^{n/p - 2}, \tag{4}$$

and

$$d^3Z/dC^3 = \sum D_n |C - C_0|^{n/p - 3}, \tag{5}$$

where

$$B_n = \pm b_n (n/p) \tag{6}$$

and

$$D_n = B_n (n - p)(n - 2p)/p^2. \tag{7}$$

Another notation convention is necessary in treating pairs of signs. In Eqs. 4 and 6, and in all the expressions to follow, the upper sign is chosen when $p = 1$ and when $p = 2$ if the expansion is about a relative minimum. The lower sign is chosen when $p = 2$ if the expansion is about a relative maximum.

The precise conditions under which Eqs. 2–5 converge is not treated here. From a computational standpoint, the inversion approach, which usually leads to an infinite number of terms in Eq. 2, is practical only if the resulting series converge rapidly. As is discussed later, the case of most interest is one in which Eq. 2 consists of a finite number of terms, N, rather than a nonterminating expansion. For a finite number of terms, there is no question of the convergence of Eqs. 2–5, and of other expansions to follow.

Before leaving the question of convergence, one should note that Eq. 2, with $p = 1$, will not suffice for the complete representation of any function for which dC/dZ vanishes in the region of interest. Consider such a function, for which $(dC/dZ)_{Z_a} = 0$, to be expanded in the form of Eq. 2 with $p = 1$ and $Z_a \neq Z_0$. Equation 2 must diverge as $C \to C_a$. In order to demonstrate this, we assume that Eq. 2 converges. If Eq. 2 converges at $C = C_a$, then, by analytic continuation, we may expand Z in a convergent Taylor's series in C about the point $C = C_a$. Such an expansion is impossible because dC/dZ is zero at $C = C_a$. It is, therefore, necessary to treat Eq. 2 for the case of $p = 2$ since one cannot represent functions

by Eq. 2 in the neighborhood of a velocity minimum or maximum by means of a convergent series with $p=1$. Since most experimental velocity profiles exhibit minima or maxima, the case of $p=2$ is of even more importance than $p=1$.

B. Expressions for Range

If the ray passes completely through a layer, the horizontal range increment in Layer i may be expressed as

$$R_i=\int_{C_i}^{C_{i+1}}\frac{C(dZ/dC)}{(C_m^2-C^2)^{\frac{1}{2}}}dC, \tag{8}$$

where C_i and C_{i+1} are the velocities at the upper and lower interfaces and C_m is the ray parameter. If the ray becomes horizontal in the layer, C_i or C_{i+1} are replaced by C_m depending, respectively, on whether the ray forms an apex or nadir. The general development to follow considers that $C_m\neq C_i$ or C_{i+1}. The case of an apex or nadir is treated under the Section on special cases.

With the use of Eq. 3, Eq. 8 may be expressed as

$$R_i=\sum B_n\int_{C_i}^{C_{i+1}}\frac{C|C-C_0|^{n/p-1}}{(C_m^2-C^2)^{\frac{1}{2}}}dC. \tag{9}$$

As is discussed in Part II, when $p=2$, the sign of odd order b_n's (and B_n's) are reversed on the two branches of the profile. Thus, in treating any integrals such as Eq. 9, it is necessary for the limits C_i and C_{i+1} to lie on the same branch of the curve. This poses little problem for, if the branch point occurs between the interfaces of interest, the integral is broken into two integrals as follows:

$$\int_{C_i}^{C_{i+1}}=\int_{C_i}^{C_0}+\int_{C_0}^{C_{i+1}}. \tag{10}$$

Each of the integrals on the right now possesses the necessary restrictions. In practice, this means that, in the representations of the profile, one must always insert an interface at any branch point.

Consider now a change of variable, $V=\pm(C-C_0)$. Equation 9 may be written as

$$R_i=\sum\bar{B}_nI_n, \tag{11}$$

where

$$\bar{B}_n=\pm C_0B_n+B_{n-p} \tag{12}$$

and

$$I_n=\int_{|C_i-C_0|}^{|C_{i+1}-C_0|}\frac{V^{n/p-1}dV}{(C_m^2-V^2\mp 2C_0V-C_0^2)^{\frac{1}{2}}}. \tag{13}$$

Expressed in terms of the original variable, Eq. 13 becomes

$$I_n=\pm\int_{C_i}^{C_{i+1}}\frac{|C-C_0|^{n/p-1}}{(C_m^2-C^2)^{\frac{1}{2}}}dC. \tag{14}$$

It should be noted that if there is a finite number of terms N in Eq. 2, the summation in Eq. 11 runs to $N+p$.

A reduction formula,[3] applied to Eq. 13, yields the recursion relation

$$\begin{aligned}I_n=[&p|C_{i+1}-C_0|^{n/p-2}(C_m^2-C_{i+1}^2)^{\frac{1}{2}}\\&-p|C_i-C_0|^{n/p-2}(C_m^2-C_i^2)^{\frac{1}{2}}\\&\pm C_0(2n-3p)I_{n-p}\\&-(C_m^2-C_0^2)(n-2p)I_{n-2p}]/(p-n).\end{aligned} \tag{15}$$

This expression is valid for $n\neq p$. Equation 15 may be used to obtain I_n for $n\geq 2p$ provided we know I_n for $n=p$ with $p=1$ or 2 and for $n=1$ and 3 with $p=2$. In the evaluation of $1\leq n<2p$, Eq. 14 is somewhat easier to treat than Eq. 13.

I_p may be represented in terms of elementary functions:

$$I_p=\pm[\cos^{-1}(C_i/C_m)-\cos^{-1}(C_{i+1}/C_m)]. \tag{16}$$

Equations 15 and 16 give the complete solution for I_n when $p=1$.

When $p=2$, I_1 and I_3 of Eq. 14 involve square roots in the integrand. These integrals can be expressed in terms of $F(\phi,k)$ and $E(\phi,k)$, the elliptic integrals of the first and second kind. It is now evident why the treatment has been limited to $p=1$ or 2. Suppose, for example, that $p=3$. Then I_1, I_2, I_4, and I_5 of Eq. 14 would involve cube roots as well as square roots in the integrand. Such integrals cannot be expressed in terms of known mathematical functions although numerical methods are a possibility.

The treatment thus far is valid regardless of the relationship of C_0 to C_i, C_{i+1}, or C_m. However, in evaluating the elliptic integrals, we must treat three cases which are determined by the relationship of C_0 to the other velocities.

1. Case 1. $C_0\leq(C_i \text{ and } C_{i+1})\leq C_m$

This is the case of an expansion about a relative minimum in velocity. The integrals are best treated by splitting into the form,

$$\int_{C_i}^{C_{i+1}}=\int_{C_i}^{C_m}-\int_{C_{i+1}}^{C_m}. \tag{17}$$

The integrals then fall under the form given by Byrd,[4] (p. 79) with I_1 under 236.00 and I_3 under 236.03. The solution is

$$I_1=(2/C_m)^{\frac{1}{2}}\bar{F}, \tag{18}$$

$$I_3=(2/C_m)^{\frac{1}{2}}[2C_m\bar{E}-(C_m+C_0)\bar{F}], \tag{19}$$

where

$$\bar{F}=F(\phi_i,k)-F(\phi_{i+1},k) \tag{20}$$

[3] G. Petit Bois, *Tables of Indefinite Integrals* (Dover Publications, Inc., New York, 1961), p. 62.

[4] P. F. Byrd and M. D. Friedman, *Handbook of Elliptic Integrals for Engineers and Physicists* (Springer-Verlag, Berlin, 1954).

and

$$\bar{E}=E(\phi_i,k)-E(\phi_{i+1},k). \tag{21}$$

We use the notation $\bar{F}$ and $\bar{E}$ throughout the treatment where ϕ_i and ϕ_{i+1} are the arguments associated with C_i and C_{i+1}, respectively, and k is the modulus. For this case,

$$k=[(C_m-C_0)/2C_m]^{\frac{1}{2}} \tag{22}$$

and

$$\phi_j=\sin^{-1}[(C_m-C_j)/(C_m-C_0)]^{\frac{1}{2}}, \quad j=i \text{ or } i+1. \tag{23}$$

For calculation purposes, it is advantageous to express $\bar{F}$ and $\bar{E}$ in terms of a single argument by means of the addition formulas given[4] under 116.01.

2. *Case* 2. C_i *and* $C_{i+1}\leq C_0\leq C_m$

This is the case of an expansion about a relative maximum in velocity and of an extended ray reaching the interface of C_0. The integrals are split into the form,

$$-\int_{C_i}^{C_{i+1}}=\int_{-C_m}^{C_i}-\int_{-C_m}^{C_{i+1}}. \tag{24}$$

The integrals fall under the form given by Byrd[4] (p. 72), with I_1 under 233.00 and I_3 under 233.04. The solution is

$$I_1=(2/C_m)^{\frac{1}{2}}\bar{F} \tag{25}$$

and

$$I_3=(2/C_m)^{\frac{1}{2}}[2C_m\bar{E}-(C_m-C_0)\bar{F}], \tag{26}$$

where

$$k=[(C_m+C_0)/2C_m]^{\frac{1}{2}} \tag{27}$$

and

$$\phi=\sin^{-1}[(C_m+C)/(C_m+C_0)]^{\frac{1}{2}}. \tag{28}$$

3. *Case* 3. C_i *and* $C_{i+1}\leq C_m\leq C_0$

This is the case of an expansion about a relative maximum in velocity and of an extended ray forming a vertex before reaching the interface of C_0. The integrals are split as in Eq. 24 and fall under forms[4] 233.00 and 233.01. The solution is

$$I_1=2(C_m+C_0)^{-\frac{1}{2}}\bar{F} \tag{29}$$

and

$$I_3=2(C_m+C_0)^{\frac{1}{2}}\bar{E}, \tag{30}$$

where

$$k=[2C_m/(C_m+C_0)]^{\frac{1}{2}} \tag{31}$$

and

$$\phi=\sin^{-1}[(C_m+C)/2C_m]^{\frac{1}{2}}. \tag{32}$$

C. Expressions for Range Derivatives

In order to obtain intensities, expressions for dR/dC_m are necessary. It is convenient to derive expressions for d^2R/dC_m^2 at the same time. Although this derivative is not required for simple ray theory intensities, it is necessary in the evaluation of the intensity at a caustic[5] and is useful in other theoretical considerations. The obvious approach is to differentiate Eqs. 15 and 16, and the various elliptic functions, i.e., Eqs. 18 and 19 or their counterparts. This leads to a relatively complicated five-term recursion relation for dI_n/dC_m. Moreover, the differentiation of the elliptic functions is complicated since both the modulus and argument are functions of C_m. An alternate approach is to differentiate Eq. 8 under the integral. This approach leads to difficulties when one of the integral limits is C_m. In this case, the integrals diverge and indeterminate forms must be treated.

These problems can be avoided by integrating Eq. 8 with respect to C by parts and then differentiating this result with respect to C_m. The result, given in Eq. 6 of Ref. 1, is

$$dR_i/dC_m=C_m\left[X_i-X_{i+1}+\int_{C_i}^{C_{i+1}}\left(\frac{d^2Z}{dC^2}\right)(C_m^2-C^2)^{-\frac{1}{2}}dC\right], \tag{33}$$

where

$$X_j=(dZ/dC)_{C_j}(C_m^2-C_j^2)^{-\frac{1}{2}}, \quad j=i \text{ or } i+1. \tag{34}$$

Similarly, an expression for d^2R_i/dC_m^2 may be obtained by integrating Eq. 33 with respect to C by parts and then differentiating this result with respect to C_m. The result is

$$d^2R_i/dC_m^2=(dR_i/dC_m)/C_m+Y_i-Y_{i+1}+\int_{C_i}^{C_{i+1}}\left(\frac{d^3Z}{dC^3}\right)\frac{C}{(C_m^2-C^2)^{\frac{1}{2}}}dC, \tag{35}$$

where

$$Y_j=(d^2Z/dC^2)_{C_j}C_j(C_m^2-C_j^2)^{-\frac{1}{2}}-C_m^2(dZ/dC)_{C_j}(C_m^2-C_j^2)^{-\frac{3}{2}}. \tag{36}$$

Substituting Eqs. 4 and 14 into Eq. 33, we obtain

$$dR_i/dC_m=C_m[X_i-X_{i+1}+\sum B_n(n-p)I_{n-p}/p]. \tag{37}$$

We may also express Eq. 37 completely in terms of B_n if we use Eq. 3 to evaluate the derivatives in Eq. 34. The result is

$$dR_i/dC_m=C_m\sum B_nJ_n, \tag{38}$$

where

$$J_n=|C_i-C_0|^{n/p-1}(C_m^2-C_i^2)^{-\frac{1}{2}}-|C_{i+1}-C_0|^{n/p-1}(C_m^2-C_{i+1}^2)^{-\frac{1}{2}}+(n-p)I_{n-p}/p. \tag{39}$$

Substituting Eqs. 5 and 14 into Eq. 35, we obtain

$$\frac{d^2R_i}{dC_m^2}=\frac{(dR_i/dC_m)}{C_m}+Y_i-Y_{i+1}+\sum\bar{D}_nI_{n-2p}, \tag{40}$$

[5] H. W. Marsh, Jr., U. S. N. Underwater Sound Lab., Tech. Memo No. 1100-61-54 (1954, unpublished).

where

$$\bar{D}_n = \pm C_0 D_n + D_{n-p}. \tag{41}$$

We may also express Eq. 40 completely in terms of B_n and $\bar{D}_n$ if we use Eqs. 3 and 4 to evaluate the derivatives in Eq. 36. The result is

$$d^2R_i/dC_m^2 = \sum B_n I_{n-p} + \sum \bar{D}_n I_{n-2p}, \tag{42}$$

where

$$\begin{aligned} L_n = J_n - C_m^2 &[(C_i - C_0)^{n/p-1}(C_m^2 - C_i^2)^{-\frac{1}{2}} \\ &- (C_{i+1} - C_0)^{n/p-1}(C_m^2 - C_{i+1}^2)^{-\frac{1}{2}}] \\ \pm &[(n-p)/p][(C_i - C_0)^{n/p-2} C_i (C_m^2 - C_i^2)^{-\frac{1}{2}} \\ &- (C_{i+1} - C_0)^{n/p-2} C_{i+1} (C_m^2 - C_{i+1}^2)^{-\frac{1}{2}}]. \end{aligned} \tag{43}$$

Expressions have already been given for I_n where $n \geq 1$. However, Eqs. 37 or 39 and 40 or 42 involve values of I_n where n ranges from 0 to -3. When $n=p$, the coefficient multiplying I_0 in Eq. 39 is zero. When $n=p$ or $n=2p$, $\bar{D}_n=0$. Hence, the coefficient multiplying I_{n-p} and I_{n-2p} in Eq. 40 or 42 is zero. The result is that I_n for $n<1$ need not be treated when $p=1$. However, when $p=2$, expressions will be needed for I_{-1} in the evaluation of Eq. 37 or 39 for $n=1$, and for I_{-1} and I_{-3} in the evaluation of Eq. 40 or 42 for $n=3$ and $n=1$.

There are two distinct approaches (each with inherent difficulties) that yield the desired expressions for dR_i/dC_m and d^2R_i/dC_m^2. The first approach is to evaluate I_{-1} and I_{-3}. This may be done by direct use of Eq. 14, utilizing type forms[4] and considering the three cases into which the integrals fall. A similar method is to utilize the recursion relation, Eq. 15. By setting $n=3$, we obtain an expression relating I_{-1} to I_3 and, by setting $n=1$, we obtain an expression relating I_{-3} to I_{-1} and I_1. However, this does not completely solve the problem. The expressions for the range derivatives contain terms that go to infinity when C_i or $C_{i+1}=C_0$. For example, the slopes in Eqs. 34 and 36 are infinite at $C_j=C_0$. Equation 37 or 38, for $n=1$, and Eq. 40 or 42, for $n=1$ and 3, are indeterminate forms of the type "infinity minus infinity." Thus, in their present form, they are not satisfactory for numerical evaluation when C_i or C_{i+1} lie in the neighborhood of C_0.

In the case of J_1, the indeterminate form can readily be reduced to

$$\begin{aligned} J_1 = \pm &[\tfrac{1}{2}(C_i - C_0)^{-\frac{1}{2}}(C_i + C_0)(C_m^2 - C_i^2)^{-\frac{1}{2}} \\ &- \tfrac{1}{2}(C_{i+1} - C_0)^{-\frac{1}{2}}(C_{i+1} + C_0)(C_m^2 - C_{i+1}^2)^{-\frac{1}{2}} \\ &\pm I_3/2](C_m^2 - C_0^2)^{-1}. \end{aligned} \tag{44}$$

Thus, when $p=2$, Eq. 44 is used in lieu of Eq. 39 for $n=1$. If the interface does not lie close to C_0, then Eq. 37 or 39 may be used, utilizing Eq. 15 to evaluate I_{-1}. Equation 37 or 39 is always used when $p=1$.

The indeterminate forms of Eq. 42 are difficult to simplify and a second approach, which is more direct, is recommended. By differentiating Eq. 11 and associating terms with B_1 from this derivative and Eq. 38, we obtain

$$J_1 = \frac{dI_3}{dC_m} - \frac{dC_m \pm C_0 dI_1}{C_m} \frac{dC_m}{dC_m}. \tag{45}$$

(One can obtain Eq. 44 from Eq. 45 by the direct differentiating of Eqs. 18 and 19 or their counterparts, although this procedure is complicated and not recommended.) We note also that the terms of d^2R/dC_m^2, as obtained by differentiating Eq. 38, associated with B_1 and B_3 are

$$B_1 J_1 + B_1 C_m dJ_1/dC_m + B_3 J_3 + B_3 C_m dJ_3/dC_m. \tag{46}$$

The derivative, dJ_1/dC_m, can be obtained in terms of J_1 and dI_1/dC_m by the differentiation of Eq. 44 and the use of Eq. 45 to eliminate dI_3/dC_m. The derivative, dJ_3/dC_m, can be obtained in terms of dI_1/dC_m by the differentiation of Eq. 39. The evaluation of Eq. 46 is then reduced to the evaluation of dI_1/dC_m. This can be done by the involved and tedious differentiation of Eq. 18 and counterparts. The appropriate expression, valid for all three cases, is

$$\begin{aligned} dI_1/dC_m = C_m^{-1}\{&[(C_i - C_0)^{\frac{1}{2}}(C_m^2 + C_0 C_i)(C_m^2 - C_i^2)^{-\frac{1}{2}} \\ &- (C_{i+1} - C_0)^{\frac{1}{2}}(C_m^2 + C_0 C_{i+1})(C_m^2 - C_{i+1}^2)^{-\frac{1}{2}} \pm C_0 I_3/2](C_m^2 - C_0^2)^{-1} - I_1/2\}. \end{aligned} \tag{47}$$

The desired result for the terms of Eq. 42 for $n=1$ and 3 becomes

$$\begin{aligned} B_1 L_1 + B_3 L_3 + \bar{D}_1 I_{-1} + \bar{D}_3 I_{-3} = {} & B_1 J_1[1 - 3C_m^2/2(C_m^2 - C_0^2)] + B_3 J_3 \\ & - C_0[B_1 C_0 J_3/(C_m^2 - C_0^2) \mp (B_1 I_1 + B_3 I_3)]/4(C_m^2 - C_0^2) \\ & + [(C_m^2 - C_0^2)B_3 \mp C_0 B_1][(C_i - C_0)^{\frac{1}{2}}(C_m^2 + C_i C_0)/(C_m^2 - C_i^2)^{\frac{1}{2}} \\ & - (C_{i+1} - C_0)^{\frac{1}{2}}(C_m^2 + C_{i+1} C_0)/(C_m^2 - C_{i+1}^2)^{\frac{1}{2}}]/2(C_m^2 - C_0^2)^2 \\ & \pm B_1 C_m^2[(C_i - C_0)^{\frac{1}{2}}(C_i + C_0)(C_m^2 - C_i^2)^{-\frac{1}{2}} \\ & - (C_{i+1} - C_0)^{\frac{1}{2}}(C_{i+1} + C_0)(C_m^2 - C_{i+1}^2)^{-\frac{1}{2}}]/(C_m^2 - C_0^2) \\ & - B_3 C_m^2[(C_i - C_0)^{\frac{1}{2}}(C_m^2 - C_i^2)^{-\frac{1}{2}} - (C_{i+1} - C_0)^{\frac{1}{2}}(C_m^2 - C_{i+1}^2)^{-\frac{1}{2}}]. \end{aligned} \tag{48}$$

Thus, when $p=2$, Eq. 42 is evaluated by omitting $n=1$ and 3 from the summation and adding Eq. 48 to the summation. It should be noted that Eq. 48 differs from Eq. 46 in the exclusion of the term $-B_3I_1$ 4, which is accounted for by Eq. 42 with $n=5$. Again, if the interface does not lie close to C_0, then Eq. 40 or 42 may be used, utilizing Eq. 15 to evaluate I_{-1} and I_{-3}. Equation 40 or 42 is always used when $p=1$.

One can verify that the indeterminate forms of Eq. 42, for $n=1$ and 3, as obtained by the first approach, can indeed be manipulated into Eq. 48. It would, however, be difficult to obtain Eq. 48 from Eq. 42 initially because of the many different ways in which the elements of Eq. 42 may be combined.

If there is a finite number of terms, N, in Eq. (2), the summation in Eq. 37 or 38 and the first summation in Eq. 42 run to N, while the summation in Eq. 40 or the second summation in Eq. 42 runs to $N+p$.

D. Expressions for Travel Time

The travel time, T_i, is given by

$$T_i=\int_{C_i}^{C_{i+1}}\frac{C_m}{C}\frac{(dZ\ dC)}{(C_m^2-C^2)^{\frac{1}{2}}}dC. \tag{49}$$

With the use of Eq. 3, Eq. 49 may be expressed

$$T_i=\sum B_nM_n, \tag{50}$$

where

$$M_n=\int_{C_i}^{C_{i+1}}\frac{C_m|C-C_0|^{n-p-1}}{C(C_m^2-C^2)^{\frac{1}{2}}}dC. \tag{51}$$

By factoring out $\pm(C-C_0)$ and dividing this factor by C, we may obtain the recursion relation,

$$M_n=C_mI_{n-p}\mp C_0M_{n-p}, \tag{52}$$

which holds for $n>p$. Since forms for I_n have already been given, the problem is reduced to the determination of M_n for $n=1$, for $p=1$ or 2, and $n=2$ for $p=2$.

When n/p is an integral value,

$$M_p=gd^{-1}\theta_i-gd^{-1}\theta_{i+1}, \tag{53}$$

where gd^{-1} is the antigudermannian function. This function is readily calculated by the series

$$gd^{-1}\theta=\sum \sin^j(\theta)/j, \tag{54}$$

where j runs over the odd integers.

When $p=2$, M_1 can be expressed in terms of $\Pi(\phi,\alpha^2,k)$, the elliptic integral of the third kind. The same cases treated for the range expression apply here.

1. *Case* 1

Equation 51 falls under form[4] 236.02. The solution is

$$M_1=(2/C_m)^{\frac{1}{2}}\bar{\Pi}, \tag{55}$$

where

$$\bar{\Pi}=\Pi(\phi_i,\alpha^2,k)-\Pi(\phi_{i+1},\alpha^2,k). \tag{56}$$

Expressions for ϕ and k have already been given and

$$\alpha^2=(C_m-C_0)/C_m. \tag{57}$$

2. *Case* 2

Equation 51 falls under form[4] 233.02. The solution is

$$M_1=(2/C_m)^{\frac{1}{2}}\bar{\Pi}, \tag{58}$$

where

$$\alpha^2=(C_m+C_0)/C_m. \tag{59}$$

3. *Case* 3

Equation 51 falls under form[4] 233.02. The solution is

$$M_1=2(C_m+C_0)^{-\frac{1}{2}}\bar{\Pi}, \tag{60}$$

where

$$\alpha^2=2. \tag{61}$$

For calculation purposes, it is advantageous for all three cases to express $\bar{\Pi}$ in terms of a single argument by means of the addition formulas given under[4] 116.02 or 116.03. For the same reason, it may also be advantageous to apply[4] 117.02 or 117.03. These latter expressions allow one to evaluate Π for values of α^2 which may be preferable to those given here. Other values of α^2, made possible by these expressions, are as follows:

Case 1: $\alpha^2=\frac{1}{2}$, $(C_0-C_m)/2C_0$, or $-C_0/C_m$;

Case 2: $\alpha^2=\frac{1}{2}$, $(C_m+C_0)/2C_0$, or C_0/C_m;

Case 3: $\alpha^2=C_m/(C_m+C_0)$, $2C_0/(C_m+C_0)$, or C_m/C_0.

In each case, the first expression for α^2 was obtained by applying 117.02, the second by applying 117.03, and the third by applying both 117.02 and 117.03.

E. Special Cases (Coincident Velocities)

The expressions for range, range derivatives, and travel time have been developed for the general case in which C_i, C_{i+1}, C_0, and C_m are all distinct. They are generally valid when some of these elements coincide, although, in some situations, certain additional conventions must be applied. Seven cases can be distinguished. For the first four cases, two of the velocities coincide. For the next two cases, three of the velocities coincide and, for the last case, all four of the velocities coincide.

1. *Case* a. $C_{i+1}<C_m\leq C_i$ *or* $C_i<C_m\leq C_{i+1}$; $C_m\neq C_0$

This is the case of a ray forming an apex or nadir. In this case, C_i or C_{i+1} are replaced by C_m. Certain terms of Eqs. 15, 16, and 53 are zero but present no problems. There appear, however, terms in Eqs. 37, 39, 40, 43, 44, and 48 which are infinite if C_m is substituted for C_i or C_{i+1}. Analysis of the derivation of Eqs. 37 or 39 and 40 or 43 show that these infinite terms arise from the differentiation of a term in the range expression (i.e., Eq. 5 of Ref. 1), which should be deleted when the

limits of integration are C_m rather than C_i or C_{i+1}. The proper procedure then is to delete all terms involving $C_m^2-C_i^2$ or $C_m^2-C_{i+1}^2$ in Eqs. 37 or 39 and 40 or 43 whenever the ray forms an apex or nadir, respectively. Furthermore, it is readily shown that these same terms in Eqs. 44 and 48 arise from terms that should be deleted in Eqs. 39, 43 and 15. Hence, these same terms should be deleted in Eqs. 44 and 48.

A further feature of interest is that ϕ_i or ϕ_{i+1} of Case 1 is zero in Eq. 23 and of Case 3 is $\pi/2$ in Eq. 32. Case 2 is not possible here.

2. *Case* b. $C_{i+1}=C_0$ *or* $C_i=C_0$; $C_m\neq C_0$

This is the case for which one of the layer interfaces coincides with the origin of the series expansion. This is an important case for $p=2$ for it has already been noted that an interface must be inserted at any branch point. Because of the development of Eqs. 44 and 48, we do not have to treat negative powers of $|C_i-C_0|$ or $|C_{i+1}-C_0|$, and this case presents no problem. Terms containing positive powers of $|C_i-C_0|$ or $|C_{i+1}-C_0|$ are zero in Eqs. 15, 39, 43, 44, and 48. Care must be taken in this case not to overlook the contribution of terms containing $|C_i-C_0|^0$ or $|C_{i+1}-C_0|^0$. Such terms occur in Eq. (15) for $n=2p$, in Eq. 39 for $n=p$, and in Eq. 43 for $n=p$ and $n=2p$. Analysis shows that $|C_i-C_0|^0$ or $|C_{i+1}-C_0|^0$ should be set equal to 1 when C_i or C_{i+1} equals C_0.

A further feature of interest is that ϕ_i or ϕ_{i+1} of Case 1 in Eq. 23 and of Case 2 in Eq. 28 are $\pi/2$. Case 3 is not possible here.

3. *Case* c. $C_{i+1}=C_0<C_m\leq C_i$ *or* $C_i=C_0<C_m\leq C_{i+1}$

This is the combination of Cases a and b and the considerations for both cases apply. Two pairs of velocities coincide. The integrals involved under Case 1 are complete elliptic integrals. A ray vertexing about an axis of minimum velocity falls into this category. Cases 2 and 3 are not possible.

4. *Case* d. $C_0=C_m\neq C_i$ *or* C_{i+1}

This is the case of a ray forming a vertex at the origin of the expansion, which does not coincide with one of the interfaces. In this case, the fourth term of Eq. 15 is zero. Thus, Eq. 15 may be used for $n>p$.

For $p=1$, this case presents no problem and is of no particular interest. For $p=2$, this case is of more interest. Cases 1 and 2 are not possible. Case 3 represents an extended ray forming a vertex at an axis of maximum velocity. In this case, the solution can be expressed solely in terms of nonelliptic functions. Evaluation of Eq. 14 leads to

$$I_1=(2/C_0)^{\frac{1}{2}}\ln\{[(C_0+C_i)^{\frac{1}{2}}+(2C_0)^{\frac{1}{2}}]\times[(C_0+C_{i+1})^{\frac{1}{2}}+(2C_0)^{\frac{1}{2}}]^{-1}\times(C_0-C_{i+1})^{\frac{1}{2}}(C_0-C_i)^{-\frac{1}{2}}\}. \quad (62)$$

Evaluation of either Eq. 14 or 15 for $n=3$ leads to

$$I_3=2[(C_0+C_i)^{\frac{1}{2}}-(C_0+C_{i+1})^{\frac{1}{2}}]. \quad (63)$$

Evaluation of Eq. 51 leads to

$$M_1=(C_0)^{-\frac{1}{2}}\ln\{[(C_0+C_i)^{\frac{1}{2}}+C_0^{\frac{1}{2}}]^2\times[(C_0+C_{i+1})^{\frac{1}{2}}+C_0^{\frac{1}{2}}]^{-2}C_{i+1}C_i^{-1}\}. \quad (64)$$

By utilizing the relations[4] of 111.04, one can show that the elliptic function representation of Eqs. 29, 30 and 60 reduce, respectively, to Eqs. 62, 63, and 64. Equations 62–64 are, then, not really necessary from a computational standpoint, although they can be used to provide a useful numerical check in the evaluation of the elliptic functions.

In contrast, Eqs. 44 and 48 are indeterminate forms of type 0/0 and are not satisfactory in their present form (from a computational standpoint). Using Eq. 15 to evaluate I_{-3} and I_{-1}, we find that

$$I_{-1}=[(C_0-C_i)^{-1}(C_0+C_i)^{\frac{1}{2}}-(C_0-C_{i+1})^{-1}(C_0+C_{i+1})^{\frac{1}{2}}+I_1/2]/2C_0 \quad (65)$$

and

$$I_{-3}=[(C_0-C_i)^{-2}(C_0+C_i)^{\frac{1}{2}}-(C_0-C_{i+1})^{-2}(C_0+C_{i+1})^{\frac{1}{2}}+3I_{-1}/2]/4C_0. \quad (66)$$

In this case, Eqs. 37 or 39 and 40 or 42 should be used, in lieu of Eqs. 44 and 48, with Eqs. 65 and 66 giving appropriate values for I_{-1} and I_{-3}.

5. *Case* e. $C_{i+1}<C_m=C_i=C_0$ *or* $C_0<C_m=C_{i+1}=C_0$

This is the case of the ray forming an apex or nadir where the ray parameter C_m is equal to C_0. For $p=1$, this case presents no problems other than those already treated under Case a. For $p=2$, Case 1 is not possible. Cases 2 and 3 represent the case of a ray vertexing at an axis of maximum velocity. This case will not be analyzed in this paper.

6. *Case* f. $C_{i+1}=C_m\leq C_i$ *or* $C_i=C_m\leq C_{i+1}$; $C_m\neq C_0$

This is the limiting case of Case a. The ray forms an apex or nadir and the ray parameter approaches the velocity of the lower or upper interface as a limit. For $p=2$, only Case 1 is possible. For Case f, one can readily show that $I_n\to 0$ for $n\geq 1$. Thus, R_i, in this case, is zero. This result states that as the ray disappears from a layer, the range in the layer goes to zero. It is also readily shown that T_i of Eq. 50 goes to zero.

Evaluation of the range derivatives for this limiting case is best accomplished from Eqs. 37 and 40. We first note that I_{-1} and I_{-3} (as well as I_n for n positive) go to zero. Thus, in the limit, Eq. 37 reduces to

$$dR_i/dC_m\to C_mX_j, \quad (67)$$

where j is $i+1$ or i depending on whether the ray forms an apex or nadir, respectively. Now $(dC/dZ)_{C_j}$ is negative or positive depending on whether the ray

forms an apex or nadir, respectively. We note also that, since $C_m \neq C_0$, $(dC/dZ)_{C_j} \neq 0$. Hence,

$$X_j \text{ and } dR_i/dC_m \rightarrow +\infty. \tag{68}$$

Similarly, by noting that the dominant term of Eq. 40 is the second term of Eq. 36, it may be shown that, in the limit,

$$d^2R_i/dC_m^2 \rightarrow -\infty. \tag{69}$$

(We note that when the ray passes through the interface, Refs. 1 and 2 prove that the infinities of Eqs. 68 and 69 are removed provided that the first and second depth derivatives of the velocity are matched at the interface.)

The results may be summarized as follows: As a ray starts to penetrate into a layer at an interface where dC/dZ is not zero, the range and travel time in the layer are zero and the range is increasing at an infinite rate, while the rate of change of range is decreasing at an infinite rate.

These results appear somewhat trivial and are what should be expected from an intuitive standpoint. However, these results are significant when contrasted to those for the case where $(dC/dZ)_{C_j}=0$.

7. *Case* g. $C_0=C_{i+1}=C_m \leq C_i$ *or* $C_0=C_i=C_m \leq C_{i+1}$

This is Case f, where the lower or upper interface is the origin of the series expansion. For $p=1$, the results stated in Case f apply. However, when $p=2$, $(dC/dZ)_{C_j}=0$ and the results are radically different than for Case f. This is the case of a ray which goes down an axis of minimum velocity. This case, which is not analyzed in this paper, and Case e, will be the subject of a subsequent paper that will analyze in depth the problem of axial rays.

F. Efficiency, Symmetry, and Separability

Several general aspects of the theoretical solution are of interest.

1. *Suitability for Programming*

The recursion procedure for generating I_n for $n \geq 2p$ and M_n for $n > p$ is well suited for programming in a high-speed digital computer. When $p=1$, the only special functions that must be computed are Eqs. 16 and 53. When $p=2$, the only special functions are Eqs. 18, 19, and 55 (or counterparts) and Eqs. 16, 53, 44, and 48. However, once these special functions have been computed, the remainder of the computation is relatively simple; for the inclusion of terms for which $N > n \geq 2p$ is just a matter of setting the proper indices in the subroutines that generate the I_n's and M_n's by recursion and those that sum the constituents of range, range derivatives, and travel time. Adding more terms to Eq. 2 merely means supplying additional profile constants as inputs and increasing the indices on the subroutines. Contrast this procedure, for example, to the extension of a two-parameter linear profile to the three-parameter curvilinear profile.[2] In this case, the addition of only one more parameter to the velocity function required a completely new program to evaluate the new expressions for range, range derivative, and travel time.

2. *Partition of Solutions*

When $p=2$, the solutions can be treated as if separated into two distinct parts—the first part consisting of terms with even n and the second part of terms with odd n. To demonstrate this, we first note that Eq. 15 expresses a relationship between I_n's for even values of n when n is even and between I_n's for odd values of n when n is odd. A similar feature holds for M_n in Eq. 52. Moreover, B_n, $\bar{B}_n$, and $\bar{D}_n$ involve b_n's for even n when n is even and b_n's for odd n when n is odd.

Thus, the first part in our partition of the solution for range, range derivative, or travel time is a function of the even b_n's, of the nonelliptic functions in Eq. 16 or 53, and of integral powers of $|C_{i+1}-C_0|$ and $|C_i-C_0|$. The first part, then, exhibits the same properties of the entire solution when $p=1$; for if $p=1$ these nonelliptic functions and integral powers are the only ones involved.

In contrast, the second part in our partition is a function of the odd b_n's, of the elliptic functions in Eqs. 18, 19, and 55 or respective counterparts, and of half-integral powers of $C_{i+1}-C_0$' and C_i-C_0'. The properties of the second part are thus quite different from those of the first part. From a numerical standpoint, the first and second parts can be computed independently because there is no interdependence.

This partition feature becomes particularly significant when treating a velocity profile that is symmetric about an axis of minimum or maximum velocity. As will be shown presently, in the case where Eq. 2 is an expansion about an axis of symmetry, $b_n=0$ for even n. In this case, the contribution of the first part of our partition is zero and the solution exhibits none of the characteristics of the nonelliptic functions and integral powers referred to previously. For example, the behavior of the ray which goes down an axis of minimum velocity is quite different for a symmetric profile as compared to some nonsymmetric profiles.

3. *Separation of Effects*

Note that the solutions consist of the summation of products where the first factor ($\bar{B}_n$, B_n, or $\bar{D}_n$) depends only on the profile parameters and is independent of the ray parameter and the limits of integration. On the other hand, the second factor (I_n, J_n, L_n, or M_n) depends on the five parameters p, C_m, C_i, C_{i+1}, and C_0, and can be regarded as almost independent of the profile. We say *almost independent* because the choice of p and the value of C_0 when $p=2$ are determined by the

profile. The important point is that the mathematical behavior of the second factor can be investigated quite independent of the profile parameters. In a sense, we have separated the effect of the basic parameters of ray theory from the effect of profile parameters.

II. THEORETICAL EXAMPLES

Part A of this Section presents the general technique for inverting analytic functions and explains how this inversion is related to our profile model of Eq. 2. Parts B–D apply the ray theory of this paper to three simple profile functions. Some of the solutions are compared with theoretical results obtained by direct methods. Parts E and F compare numerical ray-theory results, obtained by inversion or profile approximation, with corresponding results obtained by direct methods.

A. General Inversion Technique

Consider C to be an analytic function of Z at the point (Z_0,C_0). Then, C may be developed in the Taylor series

$$C-C_0=\sum a_m(Z-Z_0)^m, \tag{70}$$

where

$$a_m=(d^mC/dZ^m)_{Z_0}/m!. \tag{71}$$

It can be shown[6] that Eq. 70 may be inverted into the form

$$Z-Z_0=\sum \beta_n(C-C_0)^{n/p}, \tag{72}$$

where $a_m=0$ for $m<p$, i.e., p is the order of the first nonvanishing derivative of C with respect to Z evaluated at Z_0.

The relationship between the a_m's and the β_n's may be obtained by a tedious process of equating coefficients. A more efficient and elegant method is a generalization[7] of Lagrange's formula for the inversion of a power series.

This method expresses β_n as

$$\beta_n=1/n!\left\{\frac{d^{n-1}}{dZ^{n-1}}[\Psi(Z)]^n\right\}_{Z_0}, \tag{73}$$

where

$$\Psi(Z)=[\sum a_m(Z-Z_0)^{m-p}]^{-1/p}. \tag{74}$$

Our interest here is confined to $p=1$ or 2. The case of $p=1$ presents no problem. However, when $p=2$, we have the problem of designating the branch of the curve and also the fact that Eq. 2 differs from Eq. 72 in the use of absolute value signs.

The solution of these problems is best illustrated by the evaluation of β_n for $n\leq 5$ when $p=2$. The evaluation for higher n becomes quite involved, but the first five values suit our purpose. Evaluation of Eq. 73 results in

$$\beta_1=\mp a_2^{-\frac{1}{2}}, \tag{75}$$

$$\beta_2=-a_3/2a_2^2, \tag{76}$$

$$\beta_3=\mp\frac{a_2^{-\frac{1}{2}}\left(\frac{5a_3^2}{4a_2}-a_4\right)}{2a_2^2}, \tag{77}$$

$$\beta_4=\frac{\left(-\frac{2a_3^3}{a_2^2}+\frac{3a_3a_4}{a_2}-a_5\right)}{2a_2^3}, \tag{78}$$

and

$$\beta_5=\mp\frac{a_2^{-\frac{1}{2}}\left(\frac{231a_3^4}{64a_2^3}-\frac{63a_3^2a_4}{8a_2^2}+\frac{7a_3a_5}{2a_2}+\frac{7a_4^2}{4a_2}-a_6\right)}{2a_2^3}. \tag{79}$$

The branch of the curve is determined by the sign associated with the radical, $a_2^{-\frac{1}{2}}$. The minus sign holds for the upper branch, i.e., $Z-Z_0<0$. The plus sign holds for the lower branch, i.e., $Z-Z_0>0$. Thus, the signs of β_n for even n are the same for both branches while for odd n the signs are reversed. When a curve is symmetric about the axis, a_m is zero for odd m and β_n is zero for even n.

There remains the problem of relating the β_n of Eq. 72 to the b_n of Eq. 2. When $p=1$, the absolute value signs of Eq. 2 are removed. When $p=2$, and the expansion is about a relative minimum, the absolute-value signs may be removed without changing Eq. 2. For both these cases,

$$b_n=\beta_n. \tag{80}$$

However, when expanding about a relative maximum, $C<C_0$ and $a_2<0$. Thus, the odd powers of $(C-C_0)^{\frac{1}{2}}$ in Eq. 72 and the $(a_2)^{-\frac{1}{2}}$ appearing in β_n for odd n are pure imaginary numbers. The velocities in Eq. 72 can be made real by the use of absolute value signs. In this case,

$$\beta_n(C-C_0)^{n/2}=\beta_n(-1)^{n/2}|C-C_0|^{n/2}. \tag{81}$$

The right side of Eq. 81, reduces to Eq. 2 if

$$b_n=(-1)^{n/2}\beta_n. \tag{82}$$

Note that the b_n of Eq. 82 are all real, although β_n was pure imaginary for odd n.

B. Linear Profile

The simplest profile to treat is one for which the velocity varies linearly with depth or

$$C=C_0+g(Z-Z_0), \quad g\neq 0. \tag{83}$$

The inverse form becomes

$$Z-Z_0=(C-C_0)/g. \tag{84}$$

Evaluation of the profile parameters yields:

$p=1$; b_1, B_1, and $\bar{B}_2=g^{-1}$;

b_n and $B_n=0$ for $n>1$; $\bar{B}_1=C_0g^{-1}$;

[6] P. Dienes, *The Taylor Series* (Oxford University Press, London, 1931), p. 246.

[7] A. I. Markushevich, *Theory of Functions of A Complex Variable*, (Prentice-Hall, Inc., Englewood Cliffs, N. J., 1965), Vol. 2, p. 92.

$\bar{B}_n=0$ for $n>2$; and D_n and $\bar{D}_n=0$ for all n.
From Eq. 11,

$$R_i=C_0g^{-1}I_1+g^{-1}I_2. \tag{85}$$

Substituting Eq. 15 in Eq. 85 for I_2, we obtain

$$R_i=g^{-1}[(C_m^2-C_i^2)^{\frac{1}{2}}-(C_m^2-C_{i+1}^2)^{\frac{1}{2}}]. \tag{86}$$

From Eqs. 38 and 39,

$$dR_i/dC_m=C_mg^{-1}[(C_m^2-C_i^2)^{-\frac{1}{2}}-(C_m^2-C_{i+1}^2)^{-\frac{1}{2}}]. \tag{87}$$

From Eqs. 42 and 43,

$$d^2R_i/dC_m^2=C_m^{-1}dR_i/dC_m-C_m^2g^{-1}[(C_m^2-C_i^2)^{-\frac{3}{2}}-(C_m^2-C_{i+1}^2)^{-\frac{3}{2}}]. \tag{88}$$

From Eqs. 50 and 53,

$$T_i=g^{-1}[gd^{-1}\theta_i-gd^{-1}\theta_{i+1}]. \tag{89}$$

Equations 86–89 are readily recognized as the results obtained by elementary methods for this familiar profile.

C. Parabolic Profile

Another profile that yields a simple inversion is the parabolic profile. For this profile,

$$C=C_0+g(Z-Z_0)^2, \quad g\neq 0. \tag{90}$$

If g is negative, C_0 is a relative maximum; if g is positive, C_0 is a relative minimum. The inverse form becomes

$$Z-Z_0=l|C-C_0|^{\frac{1}{2}}, \tag{91}$$

where $l=\pm g^{-\frac{1}{2}}$. The + sign applies when $Z>Z_0$, the − sign when $Z<Z_0$.

Evaluation of the profile parameters yields:

$p=2$; $b_1=l$; B_1 and $\bar{B}_3=\pm l/2$; b_n, B_n, and $D_n=0$ for $n>1$;

$\bar{B}_1=C_0l/2$; D_1 and $\bar{D}_3=\pm 3l/8$; $\bar{D}_1=3C_0l/8$; and $\bar{B}_n$ and $\bar{D}_n=0$ for $n\neq 1$ or 3.

From Eq. 11,

$$R_i=C_0(l/2)I_1\pm(l/2)I_3. \tag{92}$$

From Eq. 38,

$$dR_i/dC_m=\pm C_mlJ_{1/2}, \tag{93}$$

where J_1 is given by Eq. 44. The quantity d^2R_i/dC_m^2 may be obtained from Eq. 48 by setting $B_1=\pm l/2$ and $B_3=0$. From Eq. 50,

$$T_i=\pm lM_1/2. \tag{94}$$

Goodman[8] investigated the range of rays forming small angles at the axis for this profile with $g=C_0\alpha^2$. The solution of this problem can be obtained from Eq. 92 with $C_m=C_{i+1}$ and $C_i=C_0$. Equation 92 reduces to

$$R_i=g|^{-\frac{1}{2}}(C_m/2)^{\frac{1}{2}}[2E(k)-K(k)], \tag{95}$$

where K and E are complete elliptic integrals of the first and second kind and the modulus k is given by Eq. 22. However, Eq. 95 represents the range from axis to vertex and must be doubled to obtain the range R from axis to vertex and back to axis. Expressed in Goodman's notation,[8] this range becomes

$$R=2R_i=2(C_m/2)^{\frac{1}{2}}[2E(k)-K(k)]/\alpha C_0^{\frac{1}{2}}. \tag{96}$$

Goodman's solution[8] applies only to low angles while Eq. 96 is the exact solution, valid for all angles.

If we now take the limit of Eq. 96 as $C_m\rightarrow C_0$, $k\rightarrow 0$, $2E(k)-K(k)\rightarrow\pi/2$, and Eq. 96 reduces to the same limit as Goodman[8] gives in his Eq. 5, which is

$$R_0=\pi/2\alpha. \tag{97}$$

D. Exponential Profile

The exponential profile yields an interesting result. For this profile,

$$C=C_0\exp[k(Z-Z_0)]. \tag{98}$$

Before examining the inversion approach, let us obtain the solution by direct methods. This is a profile for which the simplest approach[9] is integration with respect to θ. For this profile,

$$dZ=-k^{-1}\tan\theta d\theta. \tag{99}$$

If we substitute Eq. 99 into the standard expressions for range and travel time, we find that

$$R_i=-k^{-1}\int_{\theta_i}^{\theta_{i-1}}d\theta=k^{-1}(\theta-\theta_{i+1}) \tag{100}$$

and

$$T_i=-(kC_m)^{-1}\int_{\theta_i}^{\theta_{i+1}}\sec^2\theta d\theta = (kC_m)^{-1}(\tan\theta_i-\tan\theta_{i+1}). \tag{101}$$

Expressed in our parameter C_m, Eqs. 100 and 101 become

$$R_i=k^{-1}[\cos^{-1}(C_i/C_m)-\cos^{-1}(C_{i+1}/C_m)] \tag{102}$$

and

$$T_i=(kC_m)^{-1}[C_m^2-C_i^2)^{\frac{1}{2}}/C_i-(C_m^2-C_{i+1}^2)^{\frac{1}{2}}/C_{i+1}]. \tag{103}$$

The inversion is best accomplished by noting that the relationship in Eq. 98 may be expressed as

$$Z-Z_0=k^{-1}\ln(C/C_0). \tag{104}$$

By expanding $\ln(x)$ into a power series in $x-1$, we find that

$$Z-Z_0=k^{-1}[(C-C_0)/C_0-(C-C_0)^2/2C_0^2+\cdots]. \tag{105}$$

For this profile, then,

$$b_n=(-1)^{n+1}k^{-1}/nC_0^n \tag{106}$$

[8] R. R. Goodman and L. R. B. Duykers, J. Acoust. Soc. Am. 34, 960–962 (1962).

[9] Credit for this approach is due S. N. Domenico and is taken from an unpublished document.

and

$$B_n=(-1)^{n+1}k^{-1}/C_0{}^n. \tag{107}$$

From Eqs. 107 and 12, it follows that

$$\bar{B}_1=k^{-1} \quad \text{and} \quad \bar{B}_n=0 \quad \text{for} \quad n>1.$$

Equation 11 reduces to

$$R_i=k^{-1}I_1. \tag{108}$$

With the use of Eq. 16, Eq. 108 becomes Eq. 102. Thus, although there are an infinite number of terms in the inversion of the exponential profile, the range expression reduces to a single term, which is identical to that obtained by direct methods.

It should be possible to demonstrate that Eq. 50 reduces to Eq. 103 and that Eqs. 38 and 42 reduce to the expressions obtained by the differentiation of Eq. 102. However, preliminary examination has indicated that this demonstration would be quite difficult as the summations involve an infinite number of complicated terms. Thus, the occurrence of a simple result by direct methods provides no guarantee that this form of the result can readily be obtained by the inversion approach.

E. Linear Index of Refraction

In order to test the theory further, a numerical case was investigated. The three profiles just discussed were not suitable since they reduce to degenerate cases and cannot test the complete theory. The profile chosen for this numerical investigation was one with a linear index of refraction, i.e.,

$$1/C^2=1/C_0{}^2+b(Z-Z_0). \tag{109}$$

Parameters of $C_0=1640$ yd/sec, $Z=300$ yd, and $b=1.323819\times10^{-10}$ sec^{2}yd^{-3} were chosen as representative of the thermocline region of the ocean. Velocities of $C_i=1670$ yd/sec and $C_{i+1}=1630$ yd/sec were chosen, corresponding to interface depths of 200 yd and about 345 yd. The ray parameter, C_m, was chosen to be 1680 yd/sec.

The first procedure was to determine the coefficients in the inverse series. The simplest way is to note that the Taylor expansion for $y=1/C^2$ is

$$y=C_0{}^{-2}-2C_0{}^{-3}(C-C_0)+3C_0{}^{-4}(C-C_0)^2-\cdots. \tag{110}$$

By equating the right-hand sides of Eqs. 109 and 110, we find that

$$Z-Z_0=\sum b_n(C-C_0)^n, \tag{111}$$

where

$$b_n=b^{-1}(-1)^n(n+1)C_0{}^{-n-2}. \tag{112}$$

After evaluating these coefficients, the next procedure was to compare the numerical result of Eq. 111 for $C=1670$ with the value of $Z=200$ yd, as obtained from Eq. 109. This particular value was compared because it represents the largest displacement from the origin. The maximum difference between the two representations over the region of interest should occur at the maximum distance from the origin of the expansion. It is found that, by using six terms in Eq. 111, agreement to 10 significant decimal digits is achieved. However, seven terms are needed to achieve agreement of dC/dZ to 10 significant digits. This checking procedure on velocity and slopes ensures that the coefficients have been correctly evaluated, and the number of terms necessary for agreement gives an indication of the number of terms which should be employed in the ray theory summations.

Using seven terms in the summations, Eqs. 11, 38, 42, and 50 were evaluated. These numerical values were then compared with the results for the exact solution. Expressions for R_i, T_i, and dR_i/dC_m are given[10] in Eqs. 21–23. The expression for $d^2R_i/dC_m{}^2$ was obtained by the differentiation of this Eq. 23. It was found that each of the four quantities agreed with a discrepancy of only one decimal digit in the tenth significant digit. Thus, this numerical case indicates that the general approach is valid for the case of $p=1$.

One numerical problem became apparent in this study. It was found that there was considerable loss of accuracy due to roundoff in the application of Eqs. 15 and 52. In order to obtain sufficient accuracy, it appears necessary to use double-precision arithmetic in the evaluation of Eqs. 15 and 52 and of initial forms necessary in Eqs. 15 and 52, such as Eqs. 16, 18, 19, 53, and 55. After the set of I_n and M_n has been computed, the remainder of the computations may be done in single precision arithmetic.

F. Epstein Profile

A more extensive numerical test of the method for the case of $p=2$ was made using the Epstein profile as a control. The configuration of the control is discussed in detail in Ref. 2. Inversion of the Epstein profile was not attempted but rather a least-squares approximation method, to be described in Sec. III, was employed. Using Eq. 2 with 12 parameters, a least-squares fit was made to the 36 velocity-data points calculated from the Epstein profile at 3-yd intervals from the ocean surface to a depth of 105 yd. The C_0 of this fit was taken to be the axial velocity of the Epstein profile. This fit was constrained to have the same velocity, slope, and second derivative at the source depth (108 yd) as the Epstein profile has.

Figure 1 presents a critical section of the intensity curve, discussed in detail in Ref. 2. The dashed line is the intensity for the Epstein profile while the solid line is the intensity as now calculated for the 12-parameter approximation profile. Note that the curves are almost identical, the major difference being a 0.5-yd shift in the range of the caustic at a relative maximum in range. A comparison with the corresponding Figures of Ref. 2 shows that this approximation is much better than any

[10] M. A. Pedersen and D. F. Gordon, J. Acoust. Soc. Am. 37, 105–118 (1965).

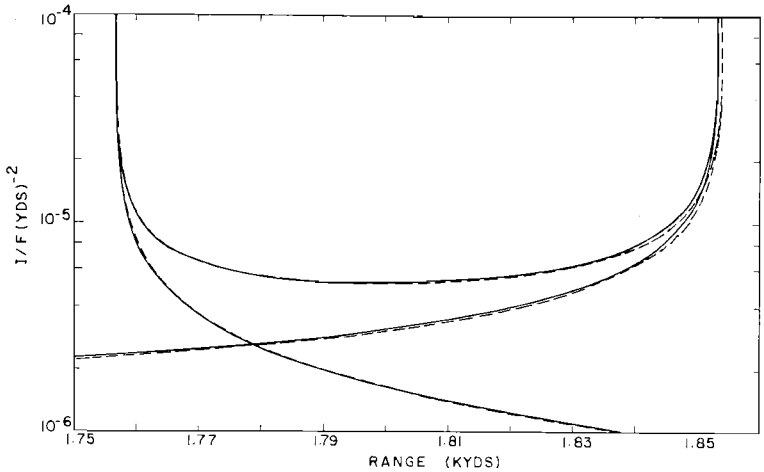

FIG. 1. Relative intensity versus range for a single layer approximation with 12 parameters (——). Epstein profile (– – –).

of those discussed in Ref. 2 and contains no artifacts despite the fact that the Ref. 2 approximations employed many more parameters. Thus, Fig. 1 not only substantiates the validity of the new approach presented here, but also indicates that this approach is definitely superior to those used heretofore that had slope or second derivative discontinuities.

In the calculation of the solid line of Fig. 1, a numerical method, employing Gaussian quadrature, rather than Eq. 15, was used to evaluate I_n for $n \geq 5$. We plan to publish a subsequent article that will discuss these improved techniques for numerical evaluation and will examine the effectiveness of the new model in more detail than can be presented here.

III. PROFILE-FITTING TECHNIQUES

This Section presents procedures which can be used to obtain the theoretical profile model from experimental velocity–depth data points. Part A treats an inversion approach, whereas Parts B and C treat a direct fit to the model for profiles with single or multiple extrema. Part D presents examples of experimental data that have been fit by the model.

A. Inversion Approach

In the inversion approach, the data points are fit by least squares to a polynomial of the form,

$$C = \sum a_n Z^n. \tag{113}$$

A difficulty encountered in this type of fit is that spurious maxima or minima may be produced. This effect can be overcome if the number of data points is sufficiently larger than the degree of the polynominal.

The next step after the polynominal has been obtained is to determine the roots of $dC/dZ = 0$, i.e., the location of the axes of minimum or maximum velocity. A series inversion is then made into Eq. 2 with $p = 2$ at each of these axes. The chief difficulty with this approach is that, although the original polynominal contains a finite number of terms, Eq. 2 contains an infinite number of terms and we are confronted with convergence problems. Each inversion will converge in some region about the point of expansion but, in general, there will be portions of the profile for which the expansion converges too slowly to be of practical use.

There may be portions of the profile which do not even lie in the regions of convergence. Thus, inversions into Eq. 2 with $p = 1$ will be necessary at additional nonaxial expansion points. With a sufficient number of these additional expansion points it is, in theory, possible to obtain inversions which "cover" the profile—i.e., there is an overlapping of the regions in which the inversions converge rapidly enough to be of practical use.

In addition to the convergence considerations of the inverted profile itself, there is the problem of the suitable convergence of all of the succeeding expansions that appear in the ray-theory development. These problems have not been investigated but, presumably, could be surmounted by sufficiently close spacing of the expansion points. Thus, in theory, it would be possible to treat a profile of the form of Eq. 113 as a single layer, provided that both first and second derivatives do not vanish simultaneously.

B. Direct Approach with One Extremum

The direct approach completely avoids convergence problems by making a least-squares fit of the data points directly to form Eq. 2. Consider first the case in which the data points indicate a single relative minimum in velocity and no relative maxima. The value for the velocity at the relative minimum, C_0, and a tentative value, Z_t, for the axial depth, Z_0, must be chosen on the basis of the data points. Let the data points be given by (Z_i, C_i). A least-squares fit of N terms is then made to the standard form

$$y = \sum_{n=0}^{N-1} b_n x^n, \tag{114}$$

where the fitted points are related to the data points by

$$y_i = Z_i \quad \text{and} \quad x_i = \pm |C_i - C_0|^{\frac{1}{2}}. \tag{115}$$

The sign of x_i is taken to be the same as that of $Z_i - Z_t$. This determination of sign is the only rôle that Z_t plays in the fitting procedure. The axial depth, Z_0, is actually determined by the least-squares fitting procedure and is given by b_0. After Z_0 has been determined, one must verify that there is no Z_i that lies between Z_t and Z_0 for, if there is, then the corresponding x_i has been estimated to lie on the wrong branch of the curve and the wrong sign has been assigned to x_i in the fitting process. If this has occurred, the fit should be repeated with a better estimate of Z_t. (Z_0 of the improper fit is probably a good candidate.) Although the choice of Z_t is not critical in the process, the choice of C_0 is. Since C_0 is contained within a radical in Eq. 115, it is not possible to determine C_0 by any simple fitting technique. One must choose the axial velocity and the resulting least-squares fit can only be good if this is a good choice.

In making the fits, the branch of the curve was indicated by the sign of the radical in Eq. 115, whereas, in Eq. 2, the branch was indicated by appropriate signs on b_n. This difference is readily reconciled by the relation

$$b_n = (\pm 1)^n \bar{b}_n, \tag{116}$$

where the plus and minus sign apply, respectively, to the deeper and shallower branch of the curve.

The same fitting approach applies if the data points indicate a single relative maximum in velocity and no relative minima.

C. Direct Approach with Multiple Extrema

Consider first the case of two extrema, i.e., the profile has both a relative minimum and maximum. In this case, two layers must be utilized. The data points are divided into two groups—Group 1 associated with the axis of maximum velocity and Group 2 with the axis of minimum velocity. The fit just discussed is made to Group 1. When this fit has been completed, the velocity and first and second depth derivatives are computed from the fit at the depth which will be the interface between the two layers. A least-squares fit is then made to the second group of points. This fit is of the form of Eq. 114 with the inclusion of Lagrange multipliers, which force the fit to match the velocity and first and second depth derivatives at the layer interface.

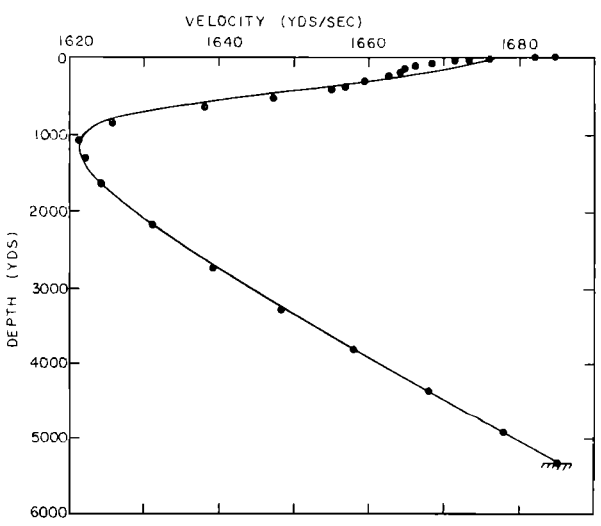

FIG. 2. A six-parameter fit to a profile with a velocity minimum.

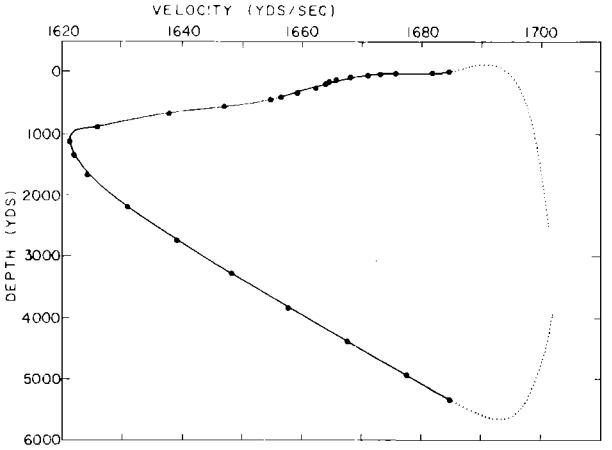

FIG. 3. A 19-parameter fit to the profile of Fig. 2. Dotted line indicates extrapolated portions.

Expressed in mathematical terms, the $\bar{b}_n$'s of the second group are determined by the system of $N+3$ equations given by

$$\partial V/\partial \bar{b}_n = 0, \quad n = 0 \text{ to } N-1 \tag{117}$$

and

$$g_m = 0, \quad m = 0 \text{ to } 2. \tag{118}$$

Here, g_m represents the side condition for matching the mth derivative at the interface, or,

$$g_m = \left\{ \frac{d^m}{dC^m} \left(\sum \bar{b}_n x^n \right) \right\}_{C_J} - \left(\frac{d^m Z}{dC_m} \right)_{C_J}. \tag{119}$$

The first term of Eq. 119 represents the derivative of the fit to be determined, evaluated at the juncture velocity (C_J). The second term of Eq. 119 represents the derivative of the fit already completed, evaluated at C_J. The function V is given by

$$V = \sum_{i=1}^{I} \left(y_i - \sum_{n=0}^{N-1} \bar{b}_n x_i^n \right)^2 + \lambda_m g_m, \tag{120}$$

where I is the number of data points in the fit, N is the number of terms in the fit, and λ_m is the Lagrangian multiplier. It is of interest to note that the coefficient matrix of the system given by Eqs. 117 and 118 is symmetric. Thus, inversion techniques that employ matrix symmetry, inherent in standard least-squares fits, may also be used here where constraints have been added to the system.

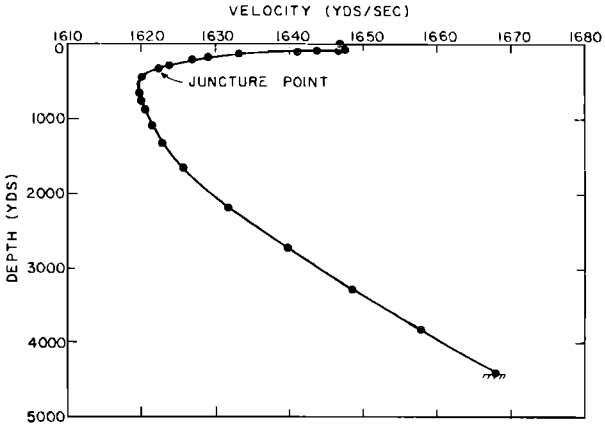

FIG. 4. A 24-parameter fit to a profile with two velocity extrema.

We believe, at present, that a matching through the second derivative will be sufficient. However, if subsequent investigation shows that discontinuities in the third- or still higher-order derivatives produce undesirable effects, such derivatives could be matched by allowing m in Eq. 118 to take on higher values in the procedure.

An alternate approach for two extrema is to make an initial fit to the points associated with the axis of minimum velocity and then fit the system given by Eqs. 117 and 118 to the points associated with the axis of maximum velocity. If more than two extrema occur in the profile, an initial fit to the form of Eq. 114 is made for the points associated with one of the extrema. Then, Eqs. 117 and 118 are applied repeatedly to connect an existing curve to data points associated with an adjacent extremum.

D. Numerical Examples

Figure 2 presents the results of the fitting procedure of Part III(B) when applied to a Pacific Ocean profile with one extremum—a velocity minimum at a depth of about 1100 yd. The dots represent the 26 data points included in the fit. Only six parameters were used in this fit ($N=5$). This fit is not particularly good since the maximum difference between the data velocity and the fit is 5.8 yd/sec. This six-parameter curve fits reasonably well below the minimum velocity but encounters difficulty in adequately fitting the steep near-surface gradient and the point of inflection, which occurs in the experimental data at a depth of about 200 yd.

Figure 3 presents the results of fitting the data points of Fig. 2 with a 19-parameter fit ($N=18$). The maximum velocity difference for this fit is 1.03 yd/sec, while the median and arithmetic average of the absolute differences are 0.14 and 0.31 yd/sec, respectively.

In Fig. 3, the dotted segments represent an extrapolation of the curve beyond the velocities at the ocean surface and ocean bottom. Both branches of the curve reverse direction. The total curve is multivalued, i.e., there is more than one value of velocity for a given value of depth. The fit is satisfactory since the curve remains single valued over the velocities of interest. It should be noted, however, that extrapolation of this type of curve beyond the velocity range of the data points is dangerous. For example, one should include in the fits a data point at the ocean bottom, in contrast to the procedure that works well in the fitting methods of Ref. 2. The procedure of Ref. 2 consists of fitting three parameter segments to data points at standard oceanographic depths above the bottom and then extrapolating to the bottom depth.

Figures 4 and 5 present the results of a fit to a Pacific Ocean profile with two extrema. The complete profile is shown in Fig. 4, while Fig. 5 presents, in more detail, the upper 600 yd of the profile. The 12 data points between the surface and 330 yd were fit by the method of Part III(B) with a 13-parameter fit. Theoretically, the curve should fit the points exactly, but, because of roundoff errors in the computer routines, there was a maximum difference between data and fit of 0.12 yd/sec. Using the method of Part III(C), an 11-parameter fit was then made to the remaining 12 data points, matching the velocity, slope, and second derivative of the first fit at a juncture point of 330 yd. The maximum difference between data and the fit was 0.14 yd/sec. The number of parameters (24) used to fit this profile may seem large. However, 46 parameters would be necessary to fit the data points exactly with straight line seg-

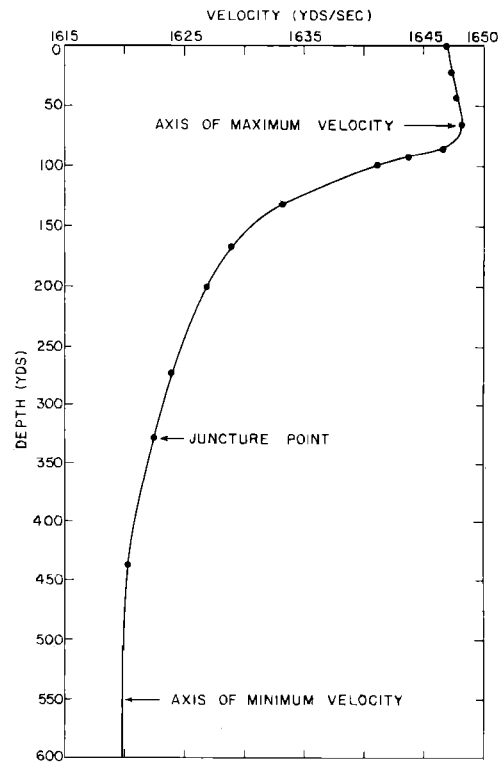

FIG. 5. The upper 600 yd of Fig. 4 in an expanded scale.

ments. The curvilinear fitting procedure of Ref. 2 is more complicated and requires 39 parameters to fit the points with an error of less than 0.25 yd/sec. Thirteen (Ref. 2) curvilinear layers are required with three parameters per layer. Thus, the methods here result in a smaller number of parameters than those of other methods with comparable accuracy.

There are two difficulties inherent in the fitting procedure—the problem of avoiding multivalued velocities over velocities of interest, and the problem of minimizing velocity differences. These difficulties are described here with possible solutions outlined in Sec. IV. Figures 6 and 7 present examples of the multivaluedness problem. Figure 6 represents a nine-parameter fit to the upper eight data points of Fig. 4. Although the curve fits the points exactly, it is unacceptable because of multiple values of C for a given depth. A similar situation holds for Fig. 7, which presents a 16-parameter fit, with constraints, to the lower 12 data points of Fig. 5.

The theoretical conditions under which a fit remains single-valued appear too complicated for practical use, so single valuedness appears to be best determined on a trial and error basis. For example, in fitting the data points of Fig. 2, fits were made and plotted for values of N between five and 18. The fits for values of N between eight and 12 were double valued. It was somewhat surprising to find that the more flexible curves for N from 13 to 18 remained single valued. The computer is programmed to calculate more than 200 points on each branch of the theoretical fit. These points then generate plots which can be visually examined for multiple values and rejected if necessary.

The second problem, involving the minimization of velocity difference between the fit and experiment, results from the fact that the least-squares technique

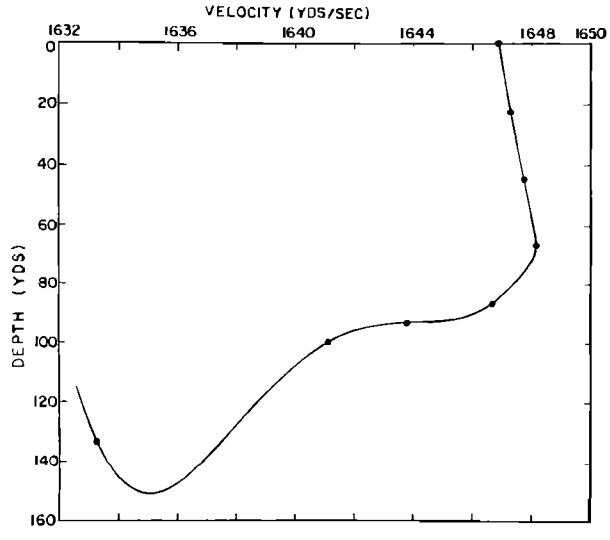

FIG. 6. An unacceptable multivalued, nine parameter fit to the upper eight data points of Fig. 5.

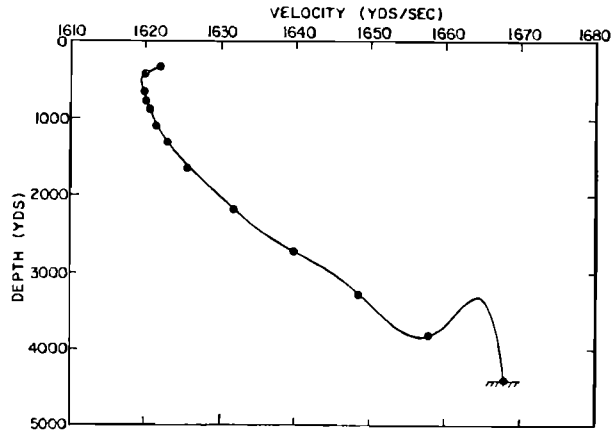

FIG. 7. An unacceptable multivalued, 16-parameter fit to the lower 13 data points of Fig. 4.

minimizes the depth differences rather than the velocity differences. Thus, in thermocline regions where the velocity gradients are large, the fit may be very good from the standpoint of minimizing depth differences for a given velocity. However, it may be rather poor from the standpoint of minimizing velocity differences for a given depth.

IV. PRESENT INVESTIGATION

Present investigation is concerned with an examination of the consequences of the general theory, with improved numerical methods for the evaluation of the integrals, and more versatile techniques for fitting velocity profiles.

Examination of the general theory is concentrating on the range and travel time of the axial ray and the associated rates of change of range, travel time, and group velocity with respect to the ray parameter. This approach provides very general answers to some of the problems that investigators[8,11–14] have sought to solve by means of very specific and simple models of the SOFAR channel.

As was previously mentioned, use of the recursion relation in the evaluation of integrals for large n can result in significant roundoff errors. An alternate method, employing numerical evaluation by Gaussian quadrature, is under investigation. This method, in some cases, is more accurate than double-precision recursion.

Various procedures for improving the accuracy of curve fitting are being developed. The curve-fitting techniques discussed in the previous section were limited to $p=2$. Improved fits can be obtained by

[11] E. T. Kornhauser, "Radiation Field of a Point Source in a Duct," U. S. Air Force Cambridge Res. Ctr. Sci. Rept. AF 4651/1 (1959).

[12] P. Hirsch and A. H. Carter, J. Acoust. Soc. Am. 37, 90–94 (1965).

[13] A. G. D. Watson, J. Acoust. Soc. Am. 40, 1202(L) (1966).

[14] D. F. Dence, J. Acoust. Soc. Am. 40, 1243(A) (1966).

inserting additional layers (with $p=1$) between the layers (with $p=2$) associated with extrema. Least-squares fits with Lagrangian multipliers are again used to fit data points and match interface conditions. This fitting procedure is simpler than for $p=2$, since polynomials, rather than radicals of $C-C_0$, are involved, and C_0 may be chosen as an arbitrary center of expansion rather than as an extremum.

Weighting factors are also being used to obtain improved fits. Here, the weighting factor used in an improved second fit is determined for each data point by the difference between the data velocity and the velocity calculated from the initial fit, i.e., points with the greatest differences receive the greatest weighting. This process may be repeated several times with significant reduction in the differences in velocity.

A technique for rectification of multivalued fits is under investigation. Suppose that, for a given value of N, a fit is multivalued over the region of interest. The set of basic data points is then augmented by realistic but fictitious data points judiciously placed so as to "pull into line" a subsequent fit to the augmented set of data points. If this subsequent fit remains multivalued or otherwise unrealistic, additional points may be placed at critical positions and the process repeated. This process of "pulling fits into line" by the addition of fictitious data points has been used successfully to treat recalcitrant cases arising in the fitting methods of Ref. 2. Addition of fictitious points is a legitimate technique provided that the resultant fits are realistic and that measurements of goodness of fit are confined to the basic data points.

V. SUMMARY

Closed form solutions for the range, travel time, and the first and second derivatives of range with respect to the ray parameter have been developed for a very general velocity-profile model in which each layer contains an arbitrary number of parameters. Any analytic velocity profile function, for which both first and second derivatures of velocity with respect to depth do not vanish simultaneously, may be cast into this model by series inversion. This method may be used to examine the mathematical profile properties upon which the ray-theory results depend.

Various techniques have been presented or outlined for fitting the velocity-profile model to experimental data points. Artifacts in acoustic fields can be minimized by the use of a few layers with many parameters and by the matching of the velocity and several derivatives at layer interfaces. Although certain practical problems in the numerical evaluation of integrals and in more accurate curve fitting have not been completely resolved, preliminary investigation indicates that the approach can be a valuable and versatile tool in the analysis of underwater sound fields by ray theory.

ACKNOWLEDGMENTS

D. F. Gordon and D. White programmed the curve fitting procedures. D. F. Gordon developed the numerical techniques and programmed the computer to obtain the results of Fig. 1. G. Wofford prepared the Figures and calculated the results for the linear index of refraction.